Effect of vesicle size on their interaction with class A amphipathic helical peptides

Jeffrey A. Gazzara,* Michael C. Phillips,† Sissel Lund-Katz,† Mayakonda N. Palgunachari,§ Jere P. Segrest,§ G.M. Anantharamaiah,§ Wendi V. Rodrigueza,† and Julian W. Snow[1,*]

Department of Chemistry,* Philadelphia College of Pharmacy and Science, Philadelphia, PA 19104; Department of Biochemistry,† Allegheny University of the Health Sciences, Philadelphia, PA 19129; and Departments of Medicine and Biochemistry and Molecular Genetics and the Atherosclerosis Research Unit,§ University of Alabama at Birmingham Medical Center, Birmingham, AL 35294

Abstract. Throughout the life span of a lipoprotein particle, the type and number of exchangeable apolipoproteins on its surface varies with particle size, suggesting a role of surface curvature on the lipid-binding properties of these proteins. Peptides 18A, Ac-18A-NH_2, Ac-18R-NH_2, 37pA, and 37aA have been designed to investigate the lipid-binding properties of the amphipathic α-helix structural motif that appears to modulate the lipid-binding properties of the exchangeable plasma apolipoproteins. We report here the results of a quantitative thermodynamic characterization of the effects of modifying helix length and of varying both the location of charged residues about the polar face of the peptides and vesicle size on the lipid affinity and depth of bilayer penetration for model amphipathic α-helices. Partition coefficients, K_p, were determined by fluorescence spectroscopy, and binding enthalpies, ΔH, by titration calorimetry. The results indicate that K_p values are on the order of 10^5, with similar ΔG° values for the interactions of the peptides with vesicles of various sizes. It appears that a class A motif and increased α-helical content optimize binding for 18-residue peptides. The interactions of the model peptides with 20 nm SUV are enthalpically driven with small, negative entropy changes; however, interactions for larger vesicles are entropically driven, likely due to disordering of bilayer hydrocarbon chains. Thermodynamic data indicate that 37pA and 37aA induce greater disordering of bilayer hydrocarbon chains than Ac-18A-NH_2. The results of this study suggest that the type of interaction, i.e., enthalpically or entropically driven, may be modulated by the lateral compressibility of the bilayer membrane.—**Gazzara, J. A., M. C. Phillips, S. Lund-Katz, M. N. Palgunachari, J. P. Segrest, G. M. Anantharamaiah, W. V. Rodrigueza, and J. W. Snow.** Effect of vesicle size on their interaction with class A amphipathic helical peptides. *J. Lipid Res.* 1997. **38:** 2147–2154.

Supplementary key words amphipathic helix • phospholipid vesicles • fluorescence • calorimetry • circular dichroism • internal bilayer tension • area compressibility

We have reported the results of a quantitative thermodynamic characterization of the interaction of five amphipathic model peptides with 20 nm small unilamellar vesicles (SUV) (1). These peptides were chosen such that the effects of varying the location of charged residues about the polar face of the helix and of modifying helix length on the lipid affinity and depth of bilayer penetration could be determined. The results indicated that the interactions constitute an enthalpically driven event which is consistent with results observed by others for interaction between highly curved phospholipid bilayers and amphipathic ligands (2, 3). The peptides 18A, Ac-18A-NH_2, Ac-18R-NH_2, 37pA, and 37aA have been designed to investigate the lipid-binding properties of the amphipathic α-helix structural motif which appears to modulate the lipid-binding properties of the exchangeable plasma apolipoproteins (4–6). Throughout the life span of a lipoprotein particle the type and number of exchangeable apolipoproteins on its surface varies with particle size, suggesting a role of particle surface curvature on the lipid-binding properties of exchangeable apolipoproteins. The size, thus degree of curvature, of a lipid particle is known to affect the lateral compressibility of the bilayer, which is inversely related to the internal tension of the bilayer (3), which is related to intermolecular potential energy between phospholipid molecules. Binding of an amphiphile to a bilayer is very likely confined to the surface in order to prevent unfavorable interactions between the hydrophobic interior of the bilayer and the hydrophilic portion of the ligand. Some penetration is ex-

Abbreviations: CD, circular dichroism; DMPC, 1,2-dimyristoyl-*sn*-glycero-3-phosphocholine; EDTA, ethylenediamine-tetraacetate; e.u., entropy units; K_p, partition coefficient; LUV, large unilamellar vesicle; MLV, multilamellar vesicles; POPC, 1-palmitoyl-2-oleoyl-*sn*-glycero-3-phosphocholine; SUV, small unilamellar vesicle.

[1]To whom correspondence should be addressed.

pected, however, of the hydrophobic portion of the ligand with resulting increases in the surface area and internal energy. An increase in lateral compressibility should minimize the increase in internal energy and therefore facilitate penetration of peptides or proteins into the bilayer (7). Also, particle size is known to affect the conformation of the apolipoprotein molecules (8). For example, apolipoprotein A-1 changes conformation as high density lipoproteins evolve from a disc into a spherical particle. However, very little is known about structural changes involved in this conformational change. Therefore the size of a lipid particle may be an important regulatory parameter in the distribution and conformation of apolipoproteins among the various classes of lipoproteins (9).

This study was performed with the synthetic phospholipid, 1-palmitoyl-2-oleoyl-*sn*-glycero-3-phosphocholine (POPC), which was used to prepare 50, 100, and 200 nm large unilamellar vesicles (LUV). Fluorescence spectroscopy was used to monitor the binding process. Ultrasensitive titration calorimetry was utilized to determine the enthalpy of interaction for the peptides at 25°C. We report here the results of a quantitative thermodynamic characterization of the effects of modifying the above-mentioned structural properties of these model peptides on their lipid affinity and depth of bilayer penetration for vesicles of different, well-defined, sizes. The results of this study suggest that the type of interaction can be either enthalpically or entropically driven, depending on vesicle size, and may be modulated by the lateral compressibility of the bilayer.

MATERIALS AND METHODS

Materials

Peptides 18A, Ac-18A-NH_2, Ac-18R-NH_2, 37pA, and 37aA were synthesized and purified by solid-phase methods as described previously (10–12). 1-Palmitoyl-2-oleoyl-*sn*-glycero-3-phosphocholine was purchased from Avanti Polar Lipids, Inc. (Alabaster, AL) and used without further purification. Sodium chloride, disodium ethylenediamine-tetraacetate (EDTA), sodium dihydrogen phosphate monohydrate, and anhydrous sodium hydrogen phosphate were purchased from Fisher Scientific Company (Fair Lawn, NJ). Acrylamide (purity $> 99.9\%$) and guanidine hydrochloride (purity $\geq 99\%$) were obtained from Bio-Rad (Richmond, CA) and Gibco BRL (Gaithersburg, MD), respectively. Indole and (1S)-(+)-10-camphorsulfonic acid were purchased from Sigma Chemical Co. (St. Louis, MO).

Preparation of peptide solutions and phospholipid vesicles

All experiments were conducted using phosphate-buffered saline (pH 7.4). Preparation of peptide solutions was performed as described previously (1). Vesicles were prepared as follows. Several aliquots of a solution of POPC in chloroform (20 mg/ml) were placed in a 15-mL Corex test tube. After each addition, the chloroform was removed under a stream of N_2, leaving a thin film of lipid on the walls of the tube. Any remaining solvent was removed by drying under vacuum at 40°C for 2 h. The dried lipid was hydrated with a 150 mM NaCl, 1 mM EDTA solution and the suspension was vortexed to generate multilamellar vesicles (MLV). Unilamellar vesicles were prepared from MLV by extrusion to produce LUV. Extrusion was carried out using a 10-mL Lipex Biomembranes Extruder equipped with a water-jacketed thermobarrel (13). MLV were sized through two stacked polycarbonate filters of defined pore size to produce 50, 100, and 200 nm vesicles (13, 14). It is important to note here that vesicles prepared by extrusion are named according to the filter pore size used in their preparation. However, typical Gaussian analyses of quasi-elastic light scattering for 50, 100, and 200 nm vesicles indicate mean diameters of 76 ± 20, 134 ± 33, and 209 ± 69 nm, respectively.

The molecular weight of the vesicles was calculated using the following formula (15)

$$MW = \frac{4\pi r_e^3 N}{3V_V} - \frac{4\pi (r_e - d)^3 N}{3\rho} \qquad Eq.\ 1)$$

where r_e is the external radius in cm, d is the bilayer thickness (2.94×10^{-7} cm), N is Avogadros number, V_V is the partial specific volume of egg phosphatidylcholine (0.9986 cm^3/g), and ρ is the specific volume of water (1 cm^3/g). The phospholipid concentration was determined spectrophotometrically by measuring the absorbance at 254 nm (ε_{254}(50 nm = 519 $M^{-1}\,cm^{-1}$; 100 nm = 1380 $M^{-1}\,cm^{-1}$; 200 nm = 2200 $M^{-1}\,cm^{-1}$)) with a Perkin-Elmer Lambda-6 spectrophotometer. This spectrophotometric assay was compared to a phosphorus assay (15) and was found to agree with it. The concentration of vesicles was calculated by dividing the concentration of lipid by the number of moles of POPC per vesicle (50 nm = 6.8×10^4; 100 nm = 2.9×10^5; 200 nm = 1.2×10^6).

Spectroscopy and calorimetry

Fluorescence spectroscopy, circular dichroism (CD), and titration calorimetry methods were performed as described previously (1).

Treatment of data

Experimental parameters determined by either nonlinear curve fitting or initial slope method were obtained using the Marquardt-Levenberg algorithm, with the SigmaPlot software package by Jandel Scientific (San Rafael, CA). The corresponding standard deviations, σ, were calculated from the standard error of the fit and the number of data points, n, from σ = standard error √n. Precision of parameters was confirmed by repeating experiments three times. Standard deviations of parameters calculated from experimental parameters were determined by calculating the propagated errors.

RESULTS

The binding isotherms in **Fig. 1** demonstrate that the normalized parameter, F_L/F_B, where F_L is the fluorescence intensity of the peptide in the presence of lipid and F_B the fluorescence intensity of the peptide in buffer, is typically saturable. However, although partitioning for the 37-residue peptides was observed with all vesicles, there is no evidence of peptide-bilayer interactions for 18A and Ac-18R-NH_2 for vesicles of any size, nor for Ac-18A-NH_2 with 200 nm vesicles. To ensure that major structural rearrangements such as disc formation were not occurring during the experiments conducted in this study, we performed gel filtration controls during which we observed no differences in migration patterns between tritiated 100-nm vesicles and peptide-vesicle complexes on a calibrated, Sepharose CL-6B column, indicating that disc formation was not occurring for representative 18-residue (Ac-18A-NH_2) or 37-residue (37pA) peptides under conditions used in these studies (peptide concentrations less than 5 μM; data not shown).

A partition model has been developed that expresses the peptide-vesicle interaction in terms of a (unitless) partition coefficient, $K_P = X_P^L/X_P^A$, the ratio of peptide mole fractions in the lipid and aqueous phases. This model has also been used to obtain stoichiometric parameters that characterize the peptide-vesicle interactions (**Table 1**). The K_P values were converted to standard free energies of partitioning, $\Delta G°$, according to $\Delta G° = -RT\ln K_P$. The K_P values obtained by fitting the data of Fig. 1 to this model (Table 1) are large, on the order of 10^5, with corresponding standard free energies of partitioning ranging from −7.5 to −8.4 kcal/mol (**Table 2**).

Stern-Volmer plots for Ac-18A-NH_2, 37pA, and 37aA complexed with 50, 100, and 200 nm POPC vesicles, in the presence of the aqueous quencher, acrylamide, are shown in **Fig. 2.** Initial slopes of these plots yield the corresponding Stern-Volmer constants for the collisional-quenching process, K_{SV}, and are given in **Table 3**. The K_{SV} values for each peptide complexed with POPC vesicles, K_{SVC}, were normalized with respect to their K_{SV} in the presence of buffer, K_{SVP}, and are given in **Table 4.** Comparison of the normalized data reveals a smaller K_{SVC}/K_{SVP} ratio for the 37-residue peptides indicating less protection against quenching for the 37-residue peptides. Also shown in Fig. 2C is the fluorescence quenching of indole, which was incorporated in the bilayer of 200 nm POPC LUV.

Calorimetric studies were conducted in order to complete the thermodynamic analysis, in which peptides were injected into excess phospholipid. Under these

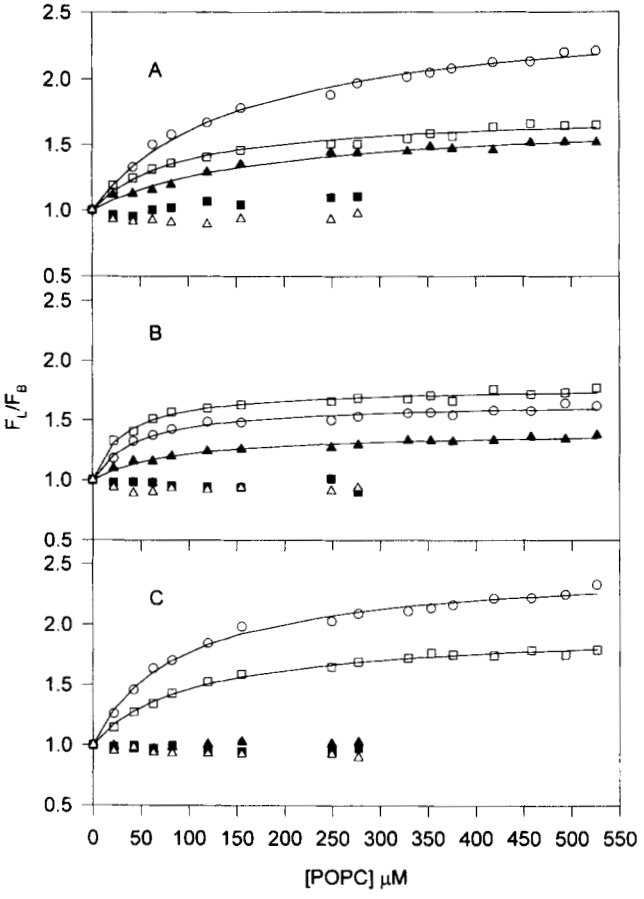

Fig. 1. Equilibrium binding isotherms for model peptides titrated with 50 nm (A), 100 nm (B), and 200 nm (C) vesicles at 25°C. The normalized fluorescence intensities, F_L/F_B, for 18A (■), Ac-18A-NH_2 (▲), Ac-18R-NH_2 (△), 37pA (□), and 37aA (○) were plotted as a function of lipid concentration. Partition coefficients, K_p, for each peptide were determined by curve fitting the respective binding isotherms (see ref. 1).

TABLE 1. Partition coefficients and lipid to peptide ratios for the partitioning of model peptides to POPC vesicles, 25°C

	Ac-18A-NH_2		37pA			37aA		
	50 nm	100 nm	50 nm	100 nm	200 nm	50 nm	100 nm	200 nm
$K_p \times 10^{-5}$[a]	3 ± 1	6 ± 3	6 ± 3	15 ± 5	5 ± 1	4 ± 1	11 ± 4	6 ± 2
Peptides per vesicle (mol/mol)[b]	190	930	220	2,730	25,570	200	2,660	25,420
Outer leaflet POPC per peptide (mol/mol)[c]	180	160	160	50	20	170	50	20

[a]Mean ± SD, number of experiments = 3.

[b]This ratio, obtained under saturating conditions, is numerically equal to $[P_L]$(POPC/vesicle)/[POPC], where $[P_L]$ is the difference between the total and free peptide concentrations, $[P] - [P_A]$.

[c]The numerator is taken to be 50% of the total [POPC]. This percentage is the ratio of the area of the outer leaflet of a sphere of a given diameter to the total area of the outer and inner leaflets. The denominator is $[P_L]$ at saturation.

conditions, peptide binding is essentially complete, allowing the observed enthalpies of interaction per mole of peptide to be determined directly. Peptides were self-associated in the syringe prior to injection, so enthalpies of peptide dissociation were determined in separate control experiments in which peptides were injected into the cell containing only buffer. As peptides were determined to be monomeric in the buffer-containing cell for reasons discussed in the previous paper (1), enthalpies of peptide-vesicle interaction were determined by subtracting the enthalpies of dissociation (control) from the observed enthalpies of interaction. We found no evidence of disc formation for peptide concentrations existing in the calorimeter cell (less than 5 μM) when we performed gel chromatography, as described above and in the previous paper (1). The standard entropies, ΔS°, of partitioning were obtained according to $\Delta S° = -(\Delta G° - \Delta H°)/T$, where it is assumed that ΔH° is approximately equal to ΔH. The thermodynamic parameters ΔH and ΔS° are summarized in Table 2.

In order to determine the α-helical content of the peptides, their far-UV CD spectra were recorded in buffer and when complexed with POPC vesicles. The results for peptides in buffer and complexed with 50, 100, and 200 nm POPC vesicles are summarized in **Table 5.** Control experiments were performed with vesicles only to determine their contribution to light scattering. These experiments indicated that scattering effects were minimal (data not shown).

DISCUSSION

In this study, a combination of isothermal titration calorimetry and fluorescence spectroscopy has provided a comprehensive set of thermodynamic parameters that characterize the interaction of Ac-18A-NH_2, 37pA, and 37aA with POPC vesicles of various size. These parameters, together with results from circular dichroism and fluorescence quenching studies, offer considerable insight regarding the molecular nature of the interaction.

As we observed previously with 20 nm SUV (1) fluorescence studies show that lipid affinities are high ($K_p \sim 10^5$, Table 1). No changes in fluorescence were observed when vesicles with diameters ranging from 50 to 200 nm were added to solutions of either 18A or Ac-18R-NH_2, suggesting a much lower affinity of these peptides for the larger vesicles. We found K_p for Ac-18A-NH_2 to be about 2 times larger for 100 nm LUV than that for 50 nm LUV, but greatest for highly curved, 20 nm SUV (1). The interactions of Ac-18A-NH_2 with vesi-

TABLE 2. Thermodynamic parameters for the partitioning of model peptides to POPC vesicles, 25°C

	Ac-18A-NH_2		37pA			37aA		
	50 nm	100 nm	50 nm	100 nm	200 nm	50 nm	100 nm	200 nm
ΔG° (kcal/mol)	−7.5 ± 0.2	−7.9 ± 0.3	−7.9 ± 0.3	−8.4 ± 0.2	−7.8 ± 0.1	−7.6 ± 0.1	−8.2 ± 0.2	−7.9 ± 0.2
H (kcal/mol)	−7.1 ± 0.3	−4.6 ± 0.6	−1.8 ± 0.5	1.0 ± 0.1	−2.2 ± 0.6	−6.3 ± 0.3	1.4 ± 0.3	2.0 ± 0.5
ΔS° (cal/mol K)	1 ± 1	11 ± 2	20 ± 2	25 ± 1	19 ± 2	4 ± 1	23 ± 1	33 ± 2

Results given as mean ± SD.

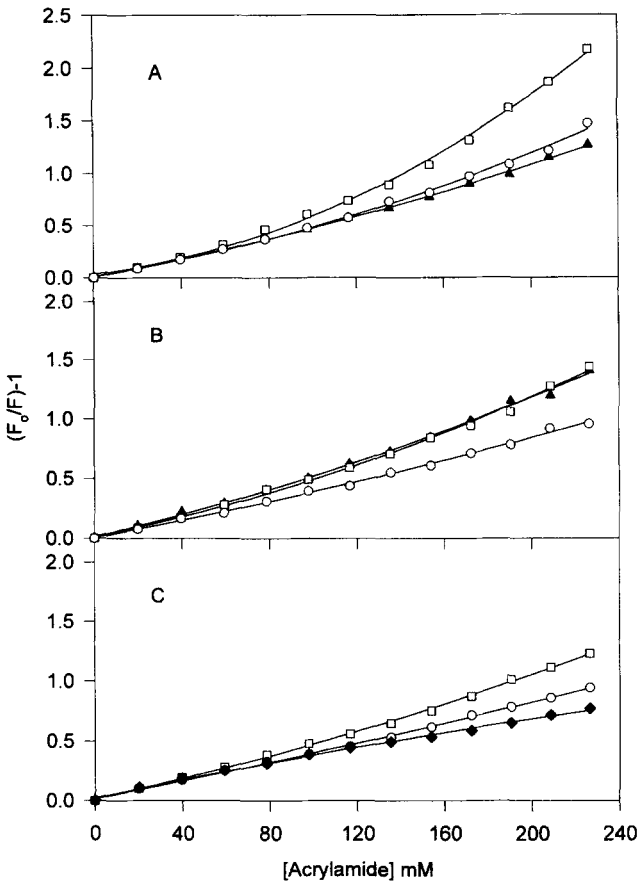

Fig. 2. Stern-Volmer plots of fluorescence quenching of the model peptides by acrylamide at 25°C complexed with 50 nm (A), 100 nm (B), and 200 nm (C) vesicles. Peptide concentration was 6 μM. The excitation wavelength was 295 nm and fluorescence intensities were measured at the emission maxima (332 nm $\leq \lambda_{max} \leq$ 360 nm). POPC/peptide molar ratios are given in Table 1. Ac-18A-NH_2 (▲), 37pA (□), 37aA (○), and Indole (◆).

cles of all sizes are found to be enthalpically and entropically favored, although the magnitude of ΔH decreases, while ΔS increases, with increasing vesicle size (Table 2). Noting also that K_p values for both 18A and Ac-18R-NH_2 for SUV are on the order of 10^5 (1), the lipid affinities of the 18-residue peptides are seen to be functions of vesicle size. That Ac-18A-NH_2 has greater lipid affinity than either 18A or Ac-18R-NH_2 for all sizes, particularly for the larger vesicles, may be due to a number of reasons. Ac-18A-NH_2 forms a class A amphipathic helix, whereas Ac-18R-NH_2 has basic and acid residues interchanged such that Lys residues are at the center and Asp and Glu residues at the edge of the polar face. The four methylene groups of the interfacial Lys residues of Ac-18A-NH_2 may provide increased van der Waals surface area (5) relative to the interfacial Asp or Glu of Ac-18R-NH_2 (one or two methylene groups, respectively), and/or there may be a more favorable interaction of the positive charges with the phosphocholine moiety of the lipid head groups of Ac-18A-NH_2 relative to negative charges (17). That Ac-18A-NH_2 has greater lipid affinity than 18A is likely due to its increased helical content, which increases the helical hydrophobic moment of the peptide (18), resulting in greater protection of its hydrophobic groups upon interaction with the bilayer.

TABLE 3. Acrylamide Stern-Volmer quenching constants of the model peptides in buffer and the model peptide-POPC complexes

	K_{SV} (M^{-1})[b]			
		POPC Complexes		
Peptide[a]	Buffer	50 nm	100 nm	200 nm
Ac-18A-NH_2	12.6 ± 0.3	4.8 ± 0.2	5.0 ± 0.4	ND
37pA	7.9 ± 0.3	5.8 ± 0.8	5.1 ± 0.6	4.8 ± 0.2
37aA	5.9 ± 0.2	4.7 ± 0.2	3.8 ± 0.4	4.2 ± 0.3
Indole	ND	ND	ND	3.9 ± 0.6

[a]Peptide concentration was 6 μM.
[b]Mean ± SD, number of experiments = 3; ND, not determined.

The data for the 37-residue peptides provide evidence that lipid affinities are a function of vesicle size and also of peptide length. Although the lipid affinities of 37pA and 37aA are not as sensitive to vesicle size as the 18-residue peptides for vesicles between 20 and 200 nm, interaction with 100-nm LUV is apparently optimal, where K_p approximately doubles. The trend in enthalpies and entropies observed for Ac-18A-NH_2 with increasing vesicle size is similar for the 37-residue peptides. Peptide-vesicle interactions are enthalpically driven for SUV with negative ΔS values; for the larger vesicles, however, the magnitude of ΔH decreases, and ΔS increases such that it is positive in all cases (Table 2). Interactions of both 37pA and 37aA with 100-nm vesicles are endothermic.

TABLE 4. Stern-Volmer quenching constants of peptide-POPC complexes relative to Stern-Volmer quenching constants of peptides in buffer

	K_{SVC}[a]/K_{SVP}[b]		
Peptide	50 nm	100 nm	200 nm
Ac-18A-NH_2	0.38 ± 0.02	0.40 ± 0.03	ND
37pA	0.7 ± 0.1	0.64 ± 0.08	0.61 ± 0.03
37aA	0.80 ± 0.04	0.64 ± 0.07	0.71 ± 0.06

[a]K_{SVC} is the Stern-Volmer quenching constant of peptide-POPC complex.
[b]K_{SVP} is the Stern-Volmer quenching constant of peptide in buffer.
Values calculated from data in Table 3, mean ± SD; ND, not determined.

TABLE 5. α-Helix content of model peptides in buffer and complexed with POPC vesicles, 25°C

	Ac-18A-NH_2		37pA			37aA		
	50 nm	100 nm	50 nm	100 nm	200 nm	50 nm	100 nm	200 nm
% Helicity buffer	38	38	26	26	26	28	28	28
% Helicity POPC complex	57	71	36	41	41	59	66	65
Δ in % helicity	19	33	10	15	15	31	38	37
Increase in number of helical residues	3.4	5.9	3.7	5.6	5.6	11.5	14.1	13.7
$\Delta S°_{\Delta Helix}$ (cal/mol K)[a]	−13.9	−24.2	−15.2	−23.0	−23.0	−47.2	−57.8	−56.2
$\Delta H_{\Delta Helix}$ (kcal/mol)[b]	−4.4	−7.7	−4.8	−7.3	−7.3	−15.0	−18.3	−17.8

[a] $\Delta S°_{\Delta Helix} = -4.1$ e.u./residue (increase in number of helical residues), see Discussion.
[b] $\Delta H_{\Delta Helix} = -1.3$ kcal/(mol of residue) (increase in number of helical residues), see Discussion.

The circular dichroism studies indicate that an increase in α-helical content occurs for all peptides upon interaction with the bilayers, with a trend for larger increases with increasing vesicle size up to 100 nm (Table 5). Increases are greatest for Ac-18A-NH_2 and 37aA (19% to 38% increases), smallest for 37pA (10% to 15% increases). Comparison of these values with their corresponding K_P values indicates that affinity is not directly related to percent helicity, which should be expected, based on reasons discussed in the previous paper (1). Increases in helicity are accompanied by decreases in both enthalpy and entropy, with the estimated magnitudes of ΔH and TΔS being approximately equal. Thus, enthalpic and entropic contributions to ΔG due to changes in helicity essentially cancel.

The fluorescence quenching data in Tables 3 and 4 for the water-soluble quencher, acrylamide, offer useful information about depths of penetration of the peptides. As in the previous paper (1), the Stern-Volmer constant for peptide-vesicle complexes, K_{SVC}, normalized to that for peptide in buffer, K_{SVP}, is taken as the most useful measure for gauging depth of bilayer penetration (Table 4). Ratios less than one indicate some measure of protection against quenching and thus against accessibility of water to the indole group of the Trp probe. The data indicate that greatest protection occurs for Ac-18A-NH_2 ($K_{SVC}/K_{SVP} = 0.38$), but also that K_{SVC} is decreased in this case by only about 60% relative to free peptide, whereas where complete burial of Trp in proteins has been shown to reduce the K_{SV} by 2 orders of magnitude (19). It is interesting to note that the K_{SV} values for indole, which should be located at the hydrocarbon-water interface (20), are similar to those for the lipid-associated peptides in this study. Protection against quenching, hence depth of bilayer penetration, appears to be greater for Ac-18A-NH_2 than for 37pA or 37aA, with little variation as a function of vesicle size from 50 to 200 nm. However, all peptides are seen to be capable of greater bilayer penetration with 20 nm SUV (1).

It is instructive to consider the molecular sources of the enthalpies and entropies of interaction listed in Tables 2 and 5. Exothermic components of enthalpy due to increases in helicity ($\Delta H_{\Delta Helix}$) have estimated magnitudes (1) ranging from 4.4 kcal/mol (Ac-18A-NH_2, 50-nm vesicles) to 18.3 kcal/mol (37aA, 100-nm vesicles). Similarly, increases in helicity lead to decreases in entropy ($\Delta S_{\Delta Helix}$), with predicted magnitudes (1) ranging from 13.9 e.u. (Ac-18A-NH_2, 50-nm vesicles) to 57.8 e.u. (37aA, 100-nm vesicles). An additional exothermic component of enthalpy would be expected due to favorable van der Waals interactions between the bilayer interior and the nonpolar faces of the peptides (2) and to net changes in electrostatic interactions ($\Delta H_{Interaction}$). Although magnitudes for $\Delta H_{Interaction}$ are difficult to determine, Seelig and Ganz (2) have pointed out that a ΔH of vaporization for benzene of ≈ +6 kcal/mol is indicative of substantial van der Waals interactions in nonpolar molecules. Peptide-phosphocholine head group (electrostatic) interactions have been shown to vary from one peptide to another (17). Peptide-lipid interaction should lead to a negative component of entropy due to a statistical effect ($\Delta S_{Interaction} < 0$).

The experimental ΔH and ΔS values in Table 2 indicate the existence of additional positive components for both. Thus, experimental ΔS values are positive in all cases; experimental ΔH values are either positive (37pA, 100 nm-vesicles, 37aA, 100- and 200-nm vesicles) or negative but with magnitudes less than expected based on $\Delta H_{\Delta Helix}$ and $\Delta H_{Interaction}$. It is likely that positive enthalpic and entropic components arise from surface effects (ΔH_{surf} and ΔS_{surf}), an idea that is supported by the fluorescence quenching results.

$$\Delta H = (-)\Delta H_{\Delta Helix} + (-)\Delta H_{Interaction} + (+)\Delta H_{Surface} \quad \textit{Eq. 2}$$

$$\Delta S = (-)\Delta S_{\Delta Helix} + (-)\Delta S_{Interaction} + (+)\Delta S_{Surface} \quad \textit{Eq. 3}$$

with the expected contribution from each component, + or −, included in parentheses.

A positive component of the enthalpy, $\Delta H_{Surface}$, may

arise from the peptide-induced area increase of the bilayer (ΔA) as the peptides partition into it (2). The origin of this positive enthalpy contribution is attributed to the internal tension of the bilayer which is defined as the variation of the internal energy, U, with surface area, A, at constant temperature. The variation of U and entropy, S, with surface area can be derived from standard thermodynamic reasoning as

$$\left(\frac{\partial U}{\partial A}\right)_T = T\left(\frac{\partial S}{\partial A}\right)_T - \pi = T\frac{\alpha}{\chi} - \pi \qquad Eq.\ 4)$$

where $\alpha = (1/A)(\partial A/\partial T)_\pi$ is defined as the area expansivity at constant membrane tension, π, and $\chi = -(1/A)(\partial A/\partial \pi)_T$ is defined as the isothermal area compressibility or lateral compressibility. As the change in volume is usually negligible for condensed phase systems (i.e., $\Delta H = \Delta U + \Delta(PV) \approx \Delta U$), Eq. 4 becomes

$$\Delta H_T \equiv \Delta H_{Surface} \approx T\frac{\alpha}{\chi}\Delta A - \pi\Delta A \qquad Eq.\ 5)$$

where ΔA is likely proportional to the area of the hydrophobic face of the peptides, and where we equate ΔH_T with ΔH_{Surf}.

The expansion of the bilayer surface, upon partitioning of the peptide, also results in an increase in entropy, perhaps due to disordering of the hydrocarbon chains induced by the increase in surface area (2). As noted in Eq. 4, $(\partial S/\partial A)_T = \alpha/\chi$, therefore

$$\Delta S_T \equiv \Delta S_{Surface} \approx \frac{\alpha}{\chi}\Delta A \qquad Eq.\ 6)$$

The area compressibility, χ, which is inversely related to vesicle size, is seen to be important in determining the nature of the peptide-lipid interactions. Small vesicles with high curvature and area compressibility have more space between adjacent phospholipid molecules than larger vesicles do. Peptides are thus more likely able to penetrate a highly curved bilayer with less displacement of phospholipid molecules, perhaps also resulting in less increase in surface area per peptide molecule. Consequently, $\Delta H_{Surface}$ and $\Delta S_{Surface}$ are small, and interactions with 20-nm SUV are dominated by negative terms in Eqs. 2 and 3, resulting in both ΔH and ΔS being negative (1). For larger vesicles, χ is smaller and the internal tension correspondingly greater. Thus, more energy is required for peptide partitioning and $\Delta H_{Surface}$ dominates Eq. 2. According to this idea, penetration of the bilayer should decrease with increasing vesicle size, which is consistent with the fluorescence results that indicate greater protection against quenching by acrylamide, hence greater penetration for SUV than for LUV (1). The binding stoichiometries (Table 1) are also consistent with the idea that penetration decreases with increasing vesicle size. The number of peptides per vesicle is seen to increase dramatically with vesicle size for all peptides, which is likely possible only if increase in area, ΔA, per peptide, hence also penetration, decreases with increasing vesicle size. For example, for partitioning of 37pA with 200 nm LUV, the peptides occupy about 1.36×10^7 Å^2, based on an interfacial area of 15 Å^2/residue occupied by α-helical peptides (21), or virtually all the 1.37×10^7 Å^2 available on a sphere of diameter 209 nm (see Methods). This increase in bilayer energy, which diminishes the importance of, or eliminates, enthalpy as a driving force for partitioning in the larger vesicles, is compensated for by a corresponding entropy increase, which dominates Eq. 3. It should be noted that Eq. 3 contains no contributions from changes in the amount of structured water in contact with hydrophobic groups. Whether water released from bound peptides rebinds to the bilayer surface or is simply not released to nearly the extent one would expect based on protein folding studies (22) is unclear. Determination of heat capacity changes could help clarify this issue. Although Wimley and White (20) observed relatively large decreases in heat capacity for partitioning of Trp side chain analogs into POPC bilayers, our initial results suggested very little temperature dependence of the heats of partitioning with 20 nm SUV.

As was mentioned previously, Ac-18A-NH_2 interacts optimally with 20 nm SUV, whereas the 37-residue peptides interact optimally with 100 nm LUV. The longer 37-residue peptides likely do not interact optimally with the highly curved surface of a 20-nm vesicle along the entire length of the peptide, despite studies that indicate that amphipathic helices may exhibit curvature due to differences in length of hydrogen bonds involving peptide backbone carbonyl oxygens, depending on whether the donor is solvent or not (23).

The model of interaction described previously in this series (1) may now be elaborated on, based on the surface effects brought to light by the studies with vesicles of varying sizes. Partitioning is confined largely to the surface of the vesicles, with only partial penetration of the amphipathic helices beyond the polar phospholipid head groups into the interior of the bilayer. Lipid affinities for the peptides are a function of vesicle size; 18-residue peptides interact optimally with SUV, whereas the 37-residue peptides, 37pA and 37aA, interact optimally with 100-nm LUV. Bilayer penetration is greatest for highly curved 20-nm vesicles with greater area compressibilities, but decreases for larger vesicles with smaller area compressibilities and greater internal energies. For small vesicles the interaction is enthalpically driven, with negative entropy changes. Relatively large components of both negative enthalpy and entropy

changes are due to increases in peptide helicity, which occur upon partitioning in all cases. With an increase in internal energy as vesicle size increases, partitioning of peptides leads to greater disordering of phospholipid acyl chains, giving rise to positive components for both enthalpy and entropy, such that for partitioning of 37-residue peptides with 100-nm vesicles, interactions are entropically driven with small endothermic components of free energies.

This research was supported in part by National Institutes of Health Program Projects HL 22633 and HL 34343.

Manuscript received 20 December 1996 and in revised form 24 June 1997.

REFERENCES

1. Gazzara, J. A., M. C. Phillips, S. Lund-Katz, M. N. Palgunachari, J. P. Segrest, G. M. Anantharamaiah, and J. W. Snow. 1997. Interaction of class A amphipathic helical peptides with phospholipid unilamellar vesicles. *J. Lipid Res.* **38:** 2134–2146.
2. Seelig, J., and P. Ganz. 1991. Calorimetric determination of enthalpy change in the α-helix to coil transition of an alanine peptide in water. *Biochemistry*. **30:** 9354–9359.
3. Beschiaschvili, G., and J. Seelig. 1992. Peptide binding to lipid bilayers. Nonclassical hydrophobic effect and membrane-induced pK shifts. *Biochemistry*. **31:** 10044–10053.
4. Segrest, J. P., R. L. Jackson, J. D. Morrisett, and A. M. Gotto, Jr. 1974. A molecular theory of lipid-protein interactions in the plasma lipoproteins. *FEBS Lett.* **38:** 247–253.
5. Segrest, J. P., H. De Loof, J. G. Dohlman, C. G. Brouillette, and G. M. Anantharamaiah. 1990. Amphipathic helix motif: classes and properties. *Proteins*. **8:** 103–117.
6. Segrest, J. P., M. K. Jones, H. De Loof, C. G. Brouillette, Y. V. Venkatachalapathi, and G. M. Anantharamaiah. 1992. The amphipathic helix in the exchangeable apolipoproteins: a review of secondary structure and function. *J. Lipid Res.* **33:** 141–166.
7. Phillips, M. C., D. E. Graham, and H. Hauser. 1975. Lateral compressibility and penetration into phospholipid monolayers and bilayer membranes. *Nature*. **254:** 154–155.
8. Jonas, A., K. E. Kezdy, and J. H. Wald. 1989. Defined apolipoprotein A-I conformation in reconstituted high density lipoprotein discs. *J. Biol. Chem.* **264:** 4818–48924.
9. Tajima, S., S. Yokoyama, and A. Yamamoto. 1983. Effect of lipid particle size on associations of apolipoproteins with lipid. *J. Biol. Chem.* **258:** 10073–10082.
10. Venkatachalapathi, Y. V., M. C. Phillips, R. M. Expand, R. F. Epand, E. M. Tytler, J. P. Segrest, and G. M. Anantharamaiah. 1993. Effect of end-group blockage on the properties of a class A amphipathic helical peptide. *Proteins*. **15:** 349–359.
11. Chung, B. H., G. M. Anantharamaiah, C. G. Brouillette, T. Nishida, and J. P. Segrest. 1985. Studies of synthetic peptide analogs of the amphipathic helix: correlation of structure with function. *J. Biol. Chem.* **260:** 10256–10262.
12. Anantharamaiah, G. M., J. L. Jones, C. G. Brouillette, C. F. Schmidt, B. H. Chung, T. A. Hughes, A. S. Bhown, and J. P. Segrest. 1985. Studies of synthetic peptide analogs of the amphipathic helix. Structures of complexes with dimyristoyl phosphatidyl choline. *J. Biol. Chem.* **260:** 10248–10255.
13. Hope, M. J., M. B. Bally, G. Webb, and P. R. Cullis. 1985. Production of large unilamellar vesicles by a rapid extrusion procedure. Characterization of size distribution, trapped volume and ability to maintain a membrane potential. *Biochim. Biophys. Acta*. **812:** 55–65.
14. Mayer, L. D., M. J. Hope, and P. R. Cullis. 1986. Vesicles of various sizes produced by a rapid extrusion procedure. *Biochim. Biophys. Acta*. **858:** 161–168.
15. McLean, L. R., and M. C. Phillips. 1982. Cholesterol desorption from clusters of phosphatidylcholine and cholesterol in unilamellar vesicle bilayers during lipid transfer or exchange. *Biochemistry*. **21:** 4053–4059.
16. Sokoloff, L., and G. H. Rothblat. 1974. Sterol to phospholipid molar ratios of L cells with qualitative and quantitative variations of cellular sterol. *Proc. Soc. Exp. Biol. Med.* **146:** 1166–1172.
17. Spuhler, P., G. M. Anantharamaiah, J. P. Segrest, and J. Seelig. 1994. Binding of apolipoprotein A-I model peptides to lipid bilayers. *J. Biol. Chem.* **269:** 23904–23910.
18. Eisenberg, D., R. M. Weiss, and T. C. Terwilliger. 1982. The helical hydrophobic moment: a measure of the amphipathicity of a helix. *Nature*. **299:** 371–374.
19. Calhoun, D. B., J. M. Vanderkooi, and S. W. Englander. 1983. Penetration of small molecules into proteins studied by quenching of phosphorescence and fluorescence. *Biochemistry*. **22:** 1533–1539.
20. Wimley, W. C., and S. H. White. 1993. Membrane partitioning: distinguishing bilayer effects from the hydrophobic effect. *Biochemistry*. **32:** 6307–6312.
21. Phillips, M. C., and K. E. Krebs. 1986. Studies of apolipoproteins at the air-water interface. *Methods Enzymol.* **128:** 387–403.
22. Tanford, C. H. 1973. The Hydrophobic Effect: Formation of Micelles and Biological Membranes. Wiley, New York. 1–3.
23. Blundell, T., D. Barlow, N. Borkakoti, and J. Thornton. 1983. Solvent-induced distortions and the curvature of α-helices. *Nature*. **306:** 281–283.